JOURNAL OF MATERIALS SCIENCE 22 (1987) 1051–1056

Nucleation and growth of aluminium oxide on silicon in the CVD process

SUNG WOO CHOI, CHUL KIM, JAE GON KIM, JOHN S. CHUN
Department of Materials Science and Engineering, Korea Advanced Institute of Science and Technology, PO Box 150, Chongryang, Seoul, Korea

Films of aluminium oxide have been formed on single crystal silicon substrates using $AlCl_3$–CO_2–H_2 gas mixtures in a cold-walled chemical vapour deposition (CVD) reactor. The nucleation and subsequent growth of the deposit have been observed under the varying process parameters. It is found that the nucleation and growth of the Al_2O_3 are dependent on the H_2O flux and H_2O supersaturation. An activation energy of 34.8 Kcal mol^{-1} is obtained for the growth rate indicating that the CVD of Al_2O_3 on silicon is a thermally activated process and limited by surface reaction. Scanning electron micrographs (SEM) show that the deposited films are amorphous at low temperature, 850° C, but change to fine grained polycrystalline structure at high temperature, 1000° C.

1. Introduction

Aluminium oxide layers, which are grown by the reaction of $AlCl_3$ with CO_2 and H_2 [1–4], are used in the electronic industry, in the fabrication of metal oxide semiconductor field effect transistors (MOSFET). The gate oxide plays an important role in MOSFET and the aluminium oxide films have been the subject of extensive investigations [2, 5, 6] because the bulk properties are better than the silicon oxide films in some respects [5]: higher dielectric strength, better radiation resistance, and impermeability to impurity diffusion.

By use of the $AlCl_3$–CO_2–H_2 system a useful non-volatile read-only memory having metal–aluminium oxide–silicon (MAS) transistors has been developed [6]. The steps of nucleation, growth of nuclei, and coalescence to form the condensed layer are important effects in understanding the deposition mechanism and surface morphology in the CVD process [7].

It is generally accepted that the factors controlling the nucleation and the resultant structures of the deposits are supersaturation and temperature [8]. The deposition temperature is an especially critical factor related to adsorbed atomic or molecular mobility, which influences the growth morphology [7–8]. In this paper we note two factors involved in nucleation: one is the deposition flux which is varied as a result of the chemical reactions among the reactant gases on the substrate, and the other factor is the supersaturation of each donor.

The present work also investigates the mechanism of the growth and resultant morphology as a function of the process parameters in the CVD of Al_2O_3.

2. Experimental procedure

2.1. Theoretical approach and calculation

The theory [9] of heterogeneous nucleation of crystals from vapour assumes that the incident atoms or molecules are adsorbed and may be diffused over the surface, and then form the critical nuclei when they join a subcritical embryo. The nucleation rate is driven by the two critical factors, the equilibrium concentration of adsorbed atoms and the supersaturation. The equilibrium concentrations of adsorbed atoms are determined by the equivalent partial pressures of the reactant gases at the surface, and the deposition flux to form a nucleus may be influenced by the variation of the concentrations of these adsorbed reactants. The supersaturation which affects the free energy of the formation of nuclei is also considered as the driving force for the nucleation in addition to the deposition flux, since these two factors are varied independently with the reactant partial pressures.

The reactant sources in this experiment can be divided into aluminium donor, $AlCl_3$ and oxygen donor, produced by the CO_2–H_2 reaction. The supersaturations of these two donors were calculated as follows

$$\Sigma_{Al} = \frac{P^{in}_{AlCl_3}}{P^{eq}_{AlCl_3} + P^{eq}_{AlCl_2} + P^{eq}_{AlCl}} \quad (1)$$

$$\Sigma_0 = \frac{P^{in}_{H_2O}}{P^{eq}_{H_2O}} \quad (2)$$

where the denominator of Equation 1 was the sum of the equilibrium partial pressures of all the aluminium chlorides (AlCl, $AlCl_2$, $AlCl_3$), since all the aluminium chlorides can contribute to the aluminium donor for Al_2O_3 [3, 4]. In Equation 2, $P^{eq}_{H_2O}$ was calculated on the assumption that the H_2O formation reaction occurs at equilibrium. The equilibrium calculations were based on the minimization of total free energy, which were accomplished by a simple iteration method [10] using a computer. The $P^{in}_{H_2O}$ was calculated by applying the values of the experimental parameters to the H_2O kinetic equation suggested by G. L. Tingey [11].

2.2. Experimental procedure

The Al_2O_3 films were deposited employing a gas

0022–2461/87 $03.00 + .12

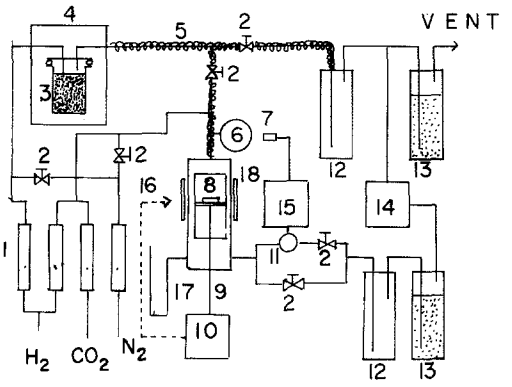

Figure 1 Experimental apparatus for chemical vapour deposition of Al_2O_3. 1, Flow meter; 2, needle valve; 3, $AlCl_3$ vaporizer; 4, temperature controller; 5, heated tube; 6, vacuum gauge; 7, optical sensor; 8, specimen; 9, thermocouple; 10, radio frequency (RF) generator; 11, solenoid valve; 12, cold trap; 13, alkali trap; 14, vacuum pump; 15, pressure controller; 16, generated RF power; 17, mercury manometer; 18, RF coil.

mixture of $AlCl_3$, CO_2 and H_2. A schematic diagram of the experimental apparatus is shown in Fig. 1. The deposition reaction took place in a cold-walled vycor glass tube with an outer diameter of 30 mm. The substrates were phosphorus-doped, single crystal silicon with (1 0 0) orientation, with dimensions of 5 × 8 × 0.2 mm.

The substrates were heated by induction and the temperatures were measured with an optical pyrometer and thermocouples. The calibrations of the flow rates of the reactant gases were accomplished at operating pressure and room temperature. The aluminium source, $AlCl_3$ vapour, was supplied by evaporation of the $AlCl_3$ solid at temperatures between 116° C and 130° C with an H_2 carrier gas. The experimental procedure can be briefly summarized as follows:

TABLE I Experimental parameters for the nucleation of Al_2O_3 (time, 3 min; total flow rate, 2 l min^{-1}; total pressure, 50 torr)

CO_2 partial pressure (torr)	$AlCl_3$ partial pressure (torr)	H_2 partial pressure (torr)	Temperature (° C)
0.75, 10 24.5, 40	0.5	48.75, 39.5 25, 9.5	950
0.75	0.15, 0.25 0.5, 1	49.1, 49.0 48.75, 48.25	950
0.75	0.5	48.75	850, 900 950, 1000

1. Before heating the reactor, the $AlCl_3$ evaporator was heated.
2. The reactor was maintained in vacuum and then purged with H_2 to prevent oxidation of the specimen during heating.
3. After the substrate reached the deposition temperature, the $AlCl_3$–H_2 and CO_2–H_2 gas mixtures flowed simultaneously into the reactor where the main reactions occurred.
4. The deposition reactions were terminated by closing the supply of $AlCl_3$ and CO_2, then the reactor was cooled in an H_2 atmosphere.

The experimental parameters and their ranges are described in Tables I and II. The surface morphology and the structure of Al_2O_3 film were analysed by scanning electron microscopy and X-ray diffraction.

3. Results and discussion

3.1. Effects of CO_2 partial pressure on the growth of Al_2O_3

Fig. 2 shows the variation of Al_2O_3 nuclei density as a function of CO_2 partial pressure in the range from 0.75 to 40 torr. Maximum nucleation rate is obtained at

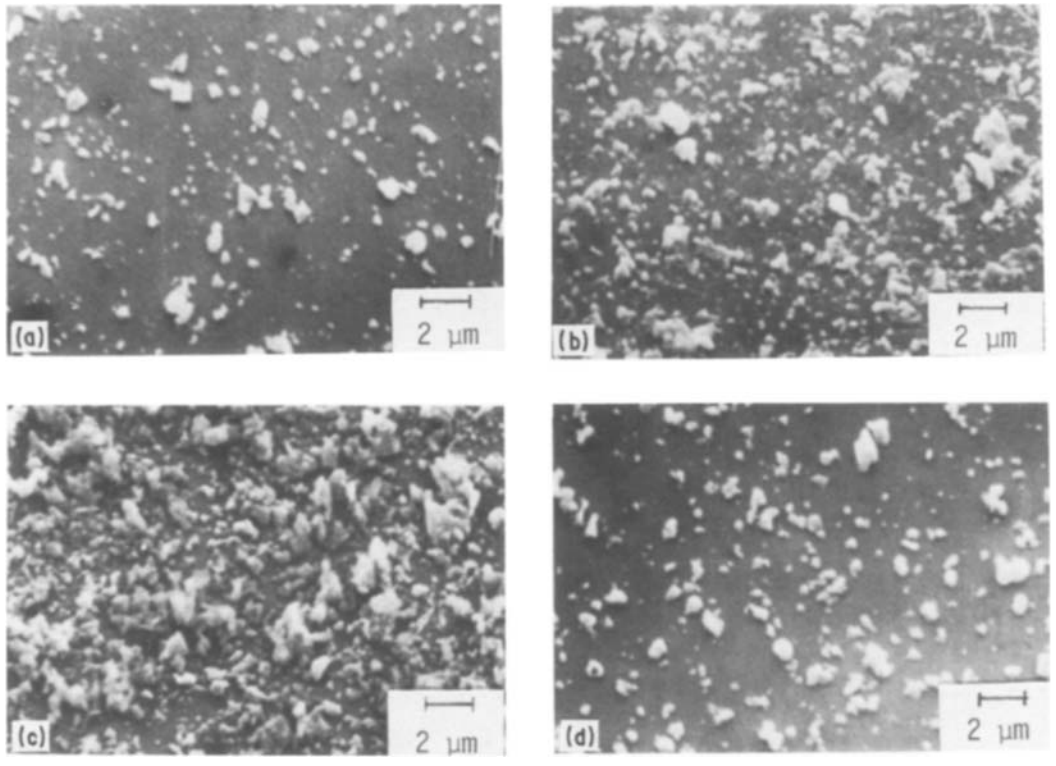

Figure 2 SEM micrographs of Al_2O_3 nucleation at different CO_2 partial pressure. (a) 0.75 torr, (b) 10 torr, (c) 24.5 torr, (d) 40 torr. (P_{AlCl_3}, 0.5 torr; total pressure, 50 torr; temperature, 950° C.)

TABLE II Experimental parameters for the growth of Al_2O_3 (time, 30 min; total flow rate, 2 l min^{-1}, total pressure, 50 torr)

CO_2 partial pressure (torr)	$AlCl_3$ partial pressure (torr)	H_2 partial pressure (torr)	Temperature (° C)
0.75, 10	0.5	48.75, 39.5	950
15, 24.5		34.5, 25	
30, 40		19.5, 9.5	
0.75	0.15, 0.25	49.1, 49	950
	0.5, 1	48.25, 48.25	
	1.5, 2	47.75, 47.25	
0.75	0.5	48.75	850, 900
			950, 1000

24.5 torr of CO_2 under the conditions of Table I (P_{AlCl_3} = 0.5 torr, P_{H_2} = 25 torr). In order to analyse this effect, we used the H_2O kinetic equation suggested by G. L. Tingey [11]. From the result of the calculations obtained by applying our experimental conditions to this equation, it is observed that the Al_2O_3 nucleation rate follows the H_2O formation rate as shown in Fig. 3. The surface concentration of H_2O is consistent with H_2O flux formed by the reaction between adsorbed molecules of CO_2 and H_2 at the surface, then the nucleation rate of Al_2O_3 may be varied as shown in Fig. 2 due to the reaction between varying H_2O and constant $AlCl_3$ content.

Fig. 4 shows the calculated supersaturations for aluminium donor and oxygen donor as a function of CO_2 partial pressure. Previous work [12] predicts that increasing supersaturation will result in an increasing nucleation rate; however, any specific supersaturation between aluminium and oxygen donors seems not to govern the Al_2O_3 nucleation from this result. Fig. 5 shows the growth rate of Al_2O_3 with increasing CO_2 partial pressure. The growth rate has a similar trend to the nucleation rate discussed above, in spite of the fact that the growth rate must have constant value within these experimental conditions (shown in Table II) with reference to the thermodynamic calculations [13].

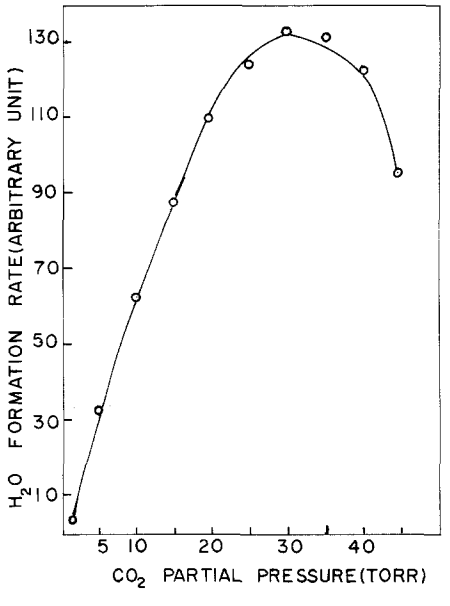

Figure 3 Calculated formation rate of H_2O as a function of CO_2 partial pressure. (P_{AlCl_3}, 0.5 torr; total pressure, 50 torr; temperature, 950° C.)

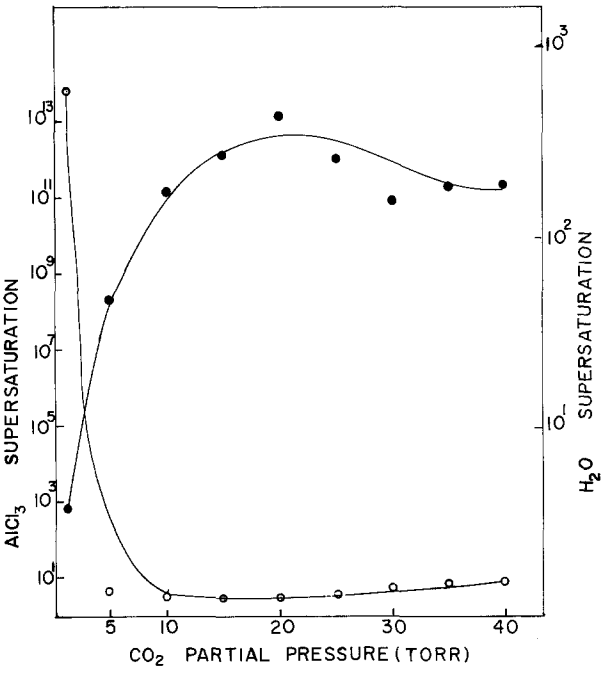

Figure 4 Calculated supersaturations as a function of CO_2 partial pressure. (P_{AlCl_3}, 0.5 torr; total pressure, 50 torr; temperature, 950° C.) ○, S_{H_2O}; ●, S_{AlCl_3}.

The reason for the discrepancy in growth rate can also be explained by the kinetics of H_2O formation. It is concluded that the kinetics of H_2O is the major limiting factor for the nucleation and growth of Al_2O_3 films.

3.2. Effects of $AlCl_3$ partial pressure on the growth of Al_2O_3

Fig. 6 shows the variation of density of Al_2O_3 nuclei as a function of $AlCl_3$ partial pressure. The nucleation rate increases with the increase of $AlCl_3$ content in the small range between 0.15 and 1 torr. Although the H_2O flux remains approximately constant under this experimental condition (P_{AlCl_3} = 0.15–1.0 torr; P_{CO_2} = 0.75 torr; P_{H_2} = 48.25–49.1 torr), the supersaturation of oxygen donor is shown to increase greatly with increasing $AlCl_3$ from Fig. 7.

We note that both the increase of $AlCl_3$ content within a small range and the H_2O supersaturation

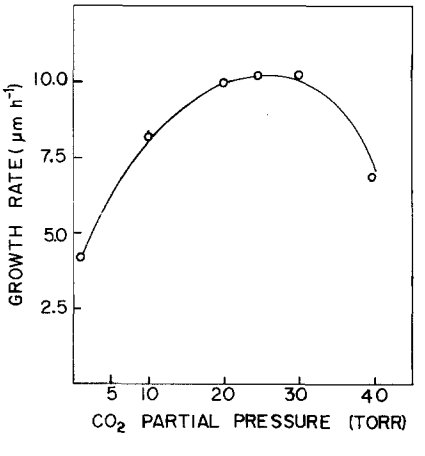

Figure 5 Growth rate of Al_2O_3 deposition as a function of CO_2 partial pressure. (P_{AlCl_3}, 0.5 torr; total pressure, 50 torr; temperature, 950° C.)

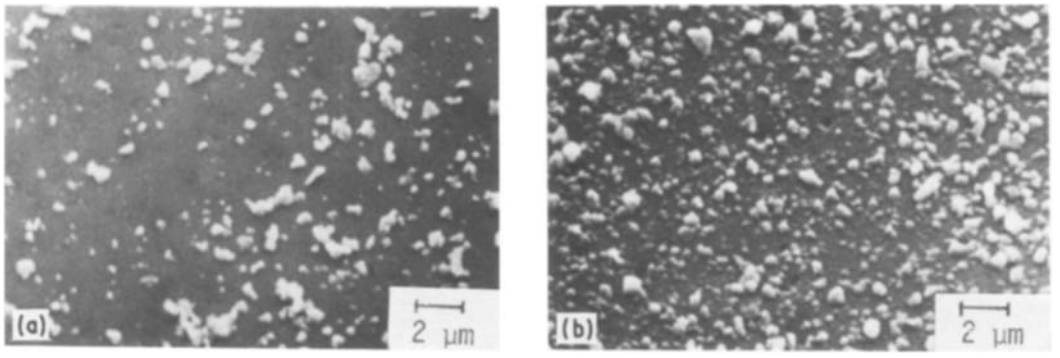

Figure 6 SEM micrographs of Al_2O_3 nucleation at different $AlCl_3$ partial pressure. (a) 0.15 torr, (b) 1 torr. (P_{CO_2}, 0.75 torr; temperature, 950° C, total pressure, 50 torr.)

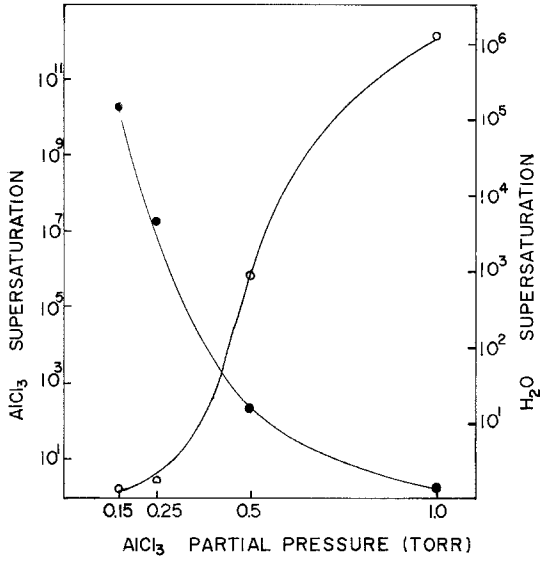

Figure 7 Calculated supersaturations as a function of $AlCl_3$ partial pressure (P_{CO_2}, 0.75 torr; temperature, 950° C; total pressure, 50 torr.) ○, S_{H_2O}; ●, S_{AlCl_3}.

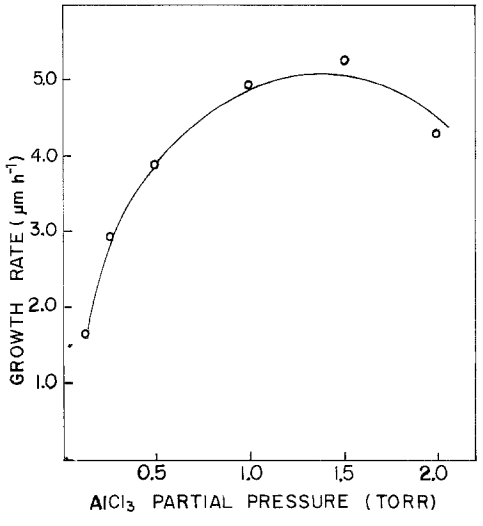

Figure 8 Growth rate of Al_2O_3 deposit as a function of $AlCl_3$ partial pressure. (P_{CO_2}, 0.75 torr; temperature, 950° C; total pressure, 50 torr.)

contribute to the Al_2O_3 nucleation. The subsequent growth phenomena after rapid occurrence of nuclei are investigated and the result is described in Fig. 8. When we consider the chemical reaction rate of Al_2O_3 to be determined by the relative amounts of aluminium and oxygen [14], the rate seems to increase due to the content of aluminium less than oxygen at $AlCl_3$ partial pressures lower than 1.5 torr, then decrease due to the content of oxygen less than aluminium at those higher than 1.5 torr.

From the results discussed above, it can be supposed that the nucleation and growth may be governed by both aluminium and oxygen donors, however, it is not clear which of the two is dominant within this experiment.

3.3. Effects of deposition temperature on the growth of Al_2O_3

Fig. 9 shows the density of nuclei as a function of deposition temperature in the range 850 to 1000° C.

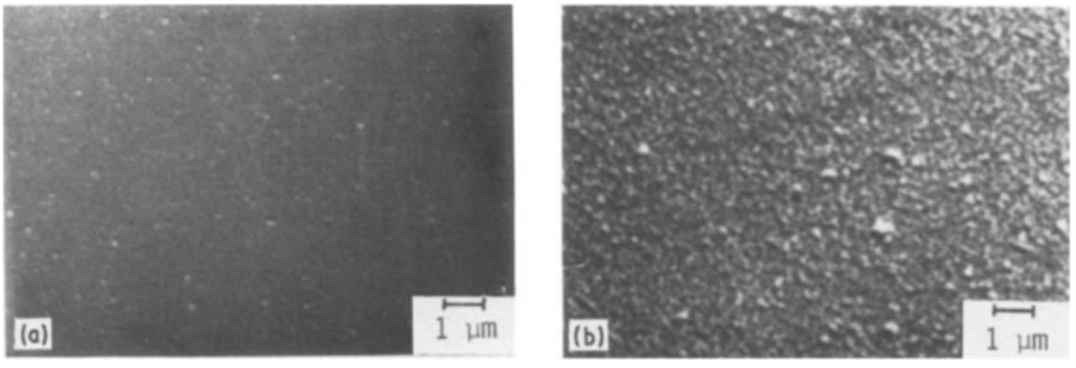

Figure 9 SEM micrographs of Al_2O_3 nucleation at different temperatures. (a) 850° C, (b) 1000° C. (P_{CO_2}, 0.75 torr; P_{AlCl_3}, 0.5 torr; P_{H_2}, 48.75 torr.)

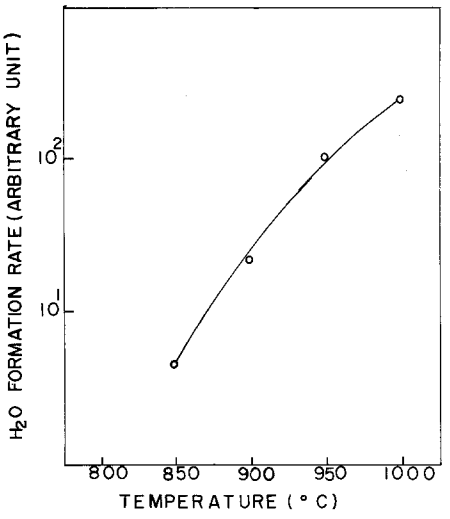

Figure 10 Calculated formation rate of H_2O as a function of temperature. (P_{CO_2}, 0.75 torr; P_{AlCl_3}, 0.5 torr; P_{H_2}, 48.75 torr.)

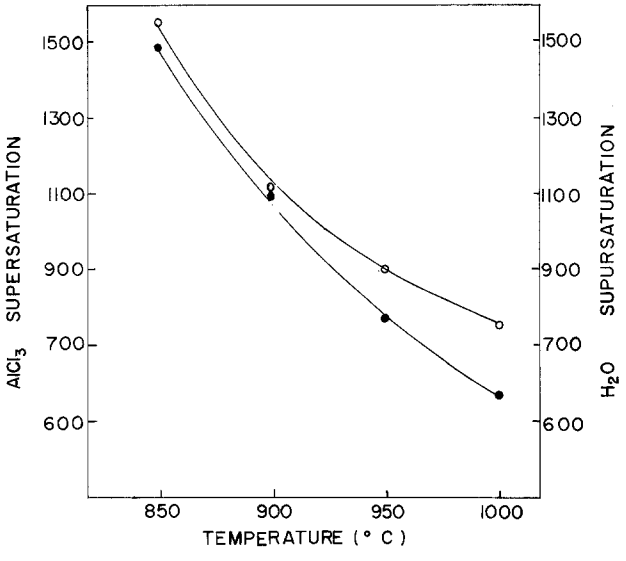

Figure 11 Calculated supersaturation as a function of deposition temperature. ○, S_{AlCl_3}; ●, S_{H_2O}. (P_{CO_2}, 0.75 torr; P_{AlCl_3}, 0.5 torr; P_{H_2}, 48.75 torr.)

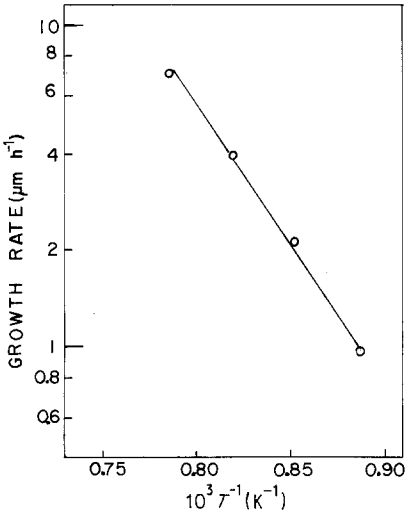

Figure 12 Temperature dependence of Al_2O_3 deposit on the growth rate. (P_{CO_2}, 0.75 torr; P_{AlCl_3}, 0.5 torr; P_{H_2}, 48.75 torr.)

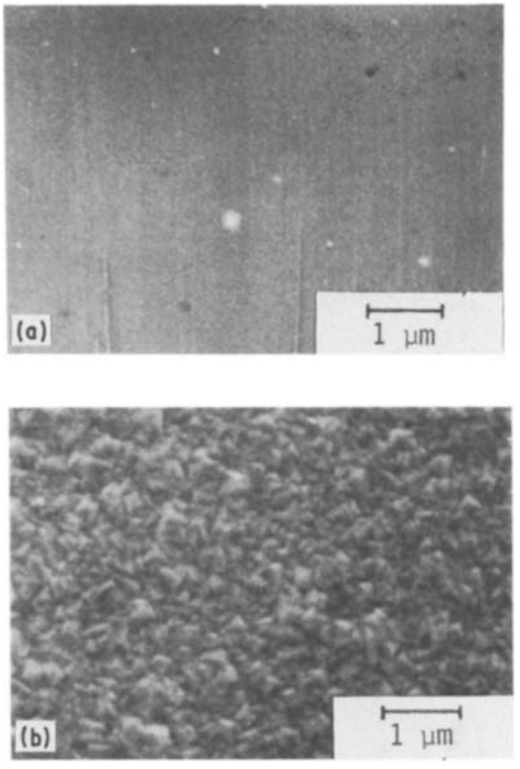

Figure 13 SEM micrographs of growth Al_2O_3 films as a function of deposition temperature. (a) 850° C, (b) 1000° C. (P_{CO_2}, 0.75 torr; P_{AlCl_3}, 0.5 torr; P_{H_2}, 48.75 torr.)

The acceleration of the nucleation rate with increasing temperature, especially the condensation of nuclei at 1000° C, is clearly observed. Despite the partial pressures of the reactant gases being kept constant, the formation of H_2O is exponentially increased as the temperature rises (see Fig. 10). We expect that the capacity to form the Al_2O_3 nuclei may be enhanced by increasing H_2O at the surface. However the supersaturations described in Fig. 11 are not likely to explain the results seen in Fig. 9, since the supersaturations of the two donors decrease. In order to determine a deposition mechanism for Al_2O_3 CVD and observe the subsequent growth morphology following nucleation, the growth rate dependence on the deposition temperature is seen in Fig. 12. A logarithmic plot of the growth rate against reciprocal of absolute temperature results in a straight line. With an activation energy of 34.8 Kcal mol^{-1} obtained from this plot, it is believed [3, 4] that the Al_2O_3 CVD on silicon is a thermally activated process and limited by surface reaction.

Fig. 13 shows the surface morphology of the grown films. The structure appears amorphous Al_2O_3 at 850° C, which suggests a deposit having insufficient atomic mobility for crystallinity at this temperature [7]. However the structure changes to a polycrystalline form, which has fine and uniform grains, at 1000° C. The X-ray diffraction analysis in Fig. 14 supports the above structural change effect as the films finally become stable α-alumina.

4. Conclusion

We note that the nucleation and growth of Al_2O_3 are closely related to H_2O forming flux and H_2O supersaturation. The CO_2 partial pressure and the

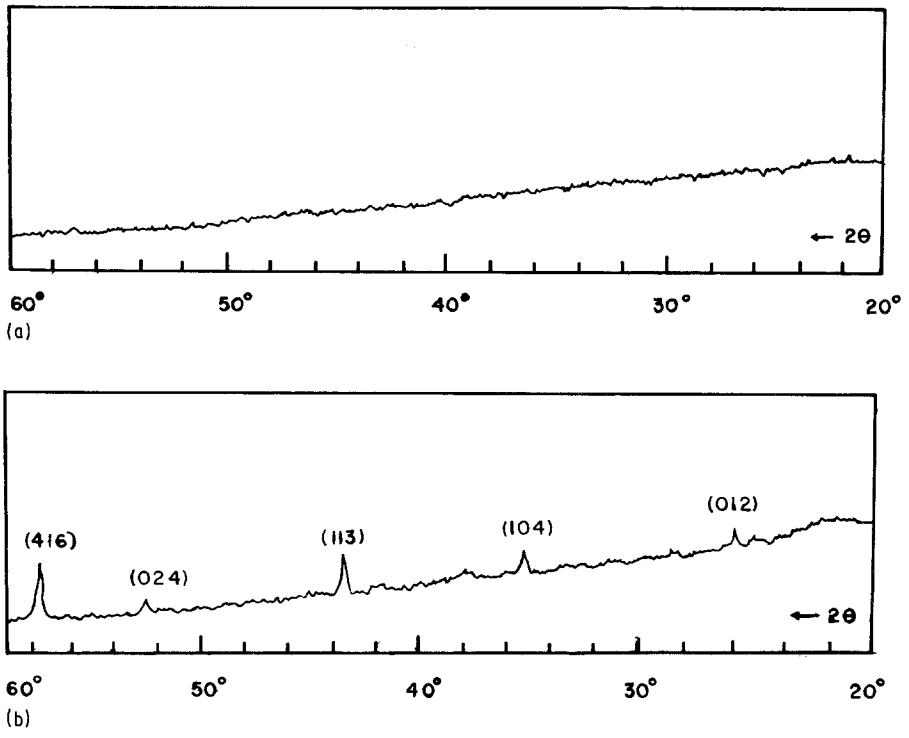

Figure 14 X-ray diffraction patterns of the deposits at different temperatures. (a) 850° C, (b) 1000° C. (P_{CO_2}, 0.75 torr; P_{AlCl_3}, 0.5 torr; P_{H_2}, 48.75 torr.)

deposition temperature, which can greatly influence H_2O formation, are the key factors in explaining the experimental results. An activation energy of 34.8 Kcal mol^{-1} is obtained, indicating that the CVD of Al_2O_3 on silicon is limited by surface reaction. SEM micrographs show that the surface morphology of the deposited films changes from amorphous to polycrystalline Al_2O_3 as the deposition temperature rises.

References

1. R. FUNK, H. SCHACHNER, C. TRIQUET and M. KORNMANN, in Proceedings of the 5th International Conference on CVD Buckinghamshire, England, 1975, (Electrochemical Society, Princeton, New Jersey, 1975) p. 469.
2. K. IIDA and T. TSUJIDE, *Jpn. J. Appl. Phys.* **11** (1972) 840.
3. J. G. KIM, C. S. PARK and J. S. CHUN, *Thin Solid Films* **97** (1982) 97.
4. C. S. PARK, J. G. KIM and J. S. CHUN, *J. Electrochem. Soc.* **130** (1983) 1607.
5. C. A. T. SALAMA, *ibid.* **117** (1970) 913.
6. S. NAKANUMA, T. TSUJDE, R. IGARASHI, K. ONODA, T. WADA and M. NAKAGIRI, *IEEE J. Solid State Circuits* **SC-5** (1970) 203.
7. J. P. HIRTH, "Vapor Deposition" (Wiley, New York, 1966) p. 126.
8. J. M. BLOCHER Jr., *J. Vac. Sci. Tech.* **11** (1974) 680.
9. G. M. POUND, M. T. SIMNAD and L. YANG, *J. Chem. Phys.* **22** (1954) 1215.
10. G. ERIKSON, *Acta Chem. Scand.* **25** (1971) 2651.
11. G. L. TINGEY, *J. Phys. Chem.* **70** (1968) 1406.
12. R. D. GRETZ, C. F. POWELL, J. H. OXLEY and J. M. BLOCHER, "Vapor Deposition" (Wiley, New York, 1966) p. 149.
13. R. COLMET and R. NASLAIN, in Proceedings of the 8th International Conference on CVD Gouvieux, France, 1981 (Electrochemical Society, Pennington, New Jersey, 1981) p. 17.
14. J. N. LINDSTRÖM and R. T. JOHANNESSON, *J. Electrochem. Soc.* **123** (1976) 854.

Received 6 May
and accepted 21 July 1986